Contents lists available at ScienceDirect

Quaternary Science Reviews

Changes in deep Pacific temperature during the mid-Pleistocene transition and Quaternary

Mark Siddall [a,*], Bärbel Hönisch [b], Claire Waelbroeck [c], Peter Huybers [d]

[a] Department of Earth Sciences, University of Bristol, Bristol, UK
[b] Lamont-Doherty Earth Observatory of Columbia University, NY 10964-8000, USA
[c] LSCE/IPSL, Laboratoire CNRS-CEA-UVSQ, Gif-sur-Yvette, France
[d] Harvard University, Cambridge, MA 02138, USA

ARTICLE INFO

ABSTRACT

An attempt is made to unravel the dual influences of seawater temperature and isotopic composition upon the oxygen-isotope records of benthic foraminifers from the deep Pacific ($\delta^{18}O_b$). Our approach is to estimate a non-linear transfer function between past sea level and $\delta^{18}O_b$ over the last two glacial cycles, with additional information from the mid-Pliocene. Combining this transfer function with the relationship between temperature and $\delta^{18}O_b$ permits a deconvolution of a $\delta^{18}O_b$ record from the deep Pacific into its temperature and sea-level constituents over the course of the Plio-Pleistocene. This deconvolution indicates that deep Pacific temperature is stable through much of the last glacial (MISs 4 through 2) and then increases by approximately 2 °C during the last deglaciation. This pattern of variability appears to generally be replicated every glacial cycle back to the mid-Pliocene, suggesting a pulse of warming in the deep Pacific on a ~100 kyr time scale during the late Pleistocene. Thus, according to this partition, there is more ~100 kyr variability in temperature than in ice variability. Spectral analysis reveals that this variability is likely the product of multiple obliquity cycles rather than a simple 100-kyr signal. The non-linear behaviour of deep ocean temperature, dominated by pulses at 100 kyr time scales, may identify it as a key player in governing the glacial cycles.

© 2009 Elsevier Ltd. All rights reserved.

1. Introduction

1.1. Mid-Pleistocene transition (MPT)

The MPT represents a reorganization of global climate during which the dominant period of climatic variability underwent a transition from the obliquity driven 41-kyr variability to variability characterised by approximately 100-kyr time scales (Pisias and Moore, 1981). A recent extensive review indicates that the MPT is a gradual transition, which began at 1250 ka BP and concluded at 700 ka BP (Clark et al., 2006). Other recent work suggests that the MPT is even more gradual and is best considered as a continuation of a long-term cooling trend (Huybers, 2007). But however abrupt or gradual this process may be, we will use the term MPT to characterise the transition from dominantly 41-kyr to approximately 100-kyr glacial variability.

There are numerous competing hypotheses to explain the MPT, including sea ice feedbacks (Tziperman and Gildor, 2003); a change in the response of ice sheets to insolation forcing under different atmospheric CO_2 forcing (Berger et al., 1999); links between the duration of ice growth and insolation forcing as a function of global temperature (Rial, 2004); the existence of multiple equilibrium states, which may be entered given a long-term cooling trend (Paillard, 1998) and changes in sediment/rock ice sheet interaction during the MPT which allowed for thicker, more voluminous ice sheets afterward (Clark and Pollard, 1998; Clark et al., 2006). Based on evidence from proxy records, several authors have suggested that changes in the East-West temperature gradients in the Pacific oceans during the MPT may indicate changes in the El Niño-Southern Oscillation (ENSO) climate modulation, which are in turn related to changes in the meridional transport of heat and water vapor in the atmosphere (Wara et al., 2005; de Garidel-Thoron et al., 2005; Lawrence et al., 2006). These authors suggest that changes in the dominant mode of ENSO variability may have a much broader impact on the glacial cycles.

Perhaps the mystery of the MPT is less the mystery of the transition than the existence of a large magnitude ~100 kyr cycle at all. Clark et al. (2006) carried out spectral analyses on a number of terrestrial and marine proxy records, noting that the '100 kyr' peak, dominant during the last 700 kyr, is in fact a broad peak

* Corresponding author.
E-mail address: mark.siddall@bristol.ac.uk (M. Siddall).

centered around 100 kyr, rather than a sharp peak, as Wunsch (2003) also pointed out. Concepts such as non-linear phase locking of ice sheet systems to relatively weak insolation forcing (Rial, 2004) or the response of ice sheets to multiple obliquity cycles (i.e. the response might be of ~80 kyr or ~ 120 kyr duration) (Huybers and Wunsch, 2005) attempt to address this question but the exact origin of the 100 kyr variability in the marine $\delta^{18}O$ records remains ambiguous as we write.

1.2. Benthic oxygen isotopes, sea level and deep-sea temperature

Oxygen isotope ratios on benthic foraminifers from ocean sediments have been measured for several decades (Emiliani, 1955). The variability in these records was initially interpreted as fluctuations in deep ocean temperature (Emiliani, 1955). However, Shackleton (1967) argued that benthic isotopes are predominantly sensitive to changes in global ice volume. A useful review is provided by Duplessy et al. (2002).

Oxygen isotope ratios show a relative depletion in the lighter isotope during glacial periods. Compared to ^{18}O, the lighter ^{16}O isotope is preferentially evaporated from the ocean. Similarly, Rayleigh distillation in the atmosphere causes strong relative enrichment of ^{16}O in high-latitude precipitation (Dansgaard, 1964). During glacial periods, growth of the large continental ice sheets leads to an increase of the $^{18}O/^{16}O$ ratio in ocean water because more of the global inventory of ^{16}O becomes locked in the ice sheets. In this way the oxygen isotope ratio in foraminifer shells is sensitive to global ice volume. It is this interpretation that has become a fundamental component of paleoclimate research, leading to a series of stratigraphic and deterministic interpretations of various benthic oxygen-isotope records in terms of ice volume (Martinson et al., 1987; Labeyrie et al., 1987; Shackleton, 2000; Raymo et al., 2006; Huybers, 2007; Lisiecki and Raymo, 2007).

Although benthic oxygen isotope ratios are an indicator of global ice volume, it is clear that deep ocean temperature variations are also a key component in the variability in the oxygen isotope ratios of benthic foraminifers. Several attempts have been made to separate the temperature and ice volume influences upon benthic oxygen isotope ratios. Chappell and Shackleton (1986) compared the benthic oxygen-isotope record from core V19-30 in the deep, equatorial Pacific with sea-level records derived from uplifted fossil coral reefs on Huon Peninsula, Papua New Guinea. These authors found that they could only reconcile the benthic oxygen-isotope record with sea-level data by assuming that deep Pacific temperature did not vary during the glacial period and was 2 °C colder than the interglacial period. Waelbroeck et al. (2002) performed a regression analysis between benthic oxygen-isotope records and sea-level estimates derived from fossil coral data for the last glacial cycle, distinguishing between the North Atlantic and Pacific Ocean as well as between the glacial inception and termination, in an attempt to account for temporal and spatial variability in the relationship. The regression results were used along with benthic oxygen-isotope records from each of the ocean basins to calculate sea-level and temperature variations for the last four glacial cycles. Cutler et al. (2003) followed the approach of Chappell and Shackleton (1986), in which sea-level records are generated through scaling benthic oxygen-isotope records using fossil coral data. In particular, Cutler et al. (2003) used new and previously published U/Th dates, to generate a set of coral-based age versus sea-level estimates which was in turn used to scale benthic oxygen-isotope records from equatorial Pacific core V19-30 and Atlantic core EW9209-1 in terms of sea-level. After subtracting the sea-level contribution, residual oxygen isotope ratios were interpreted to reflect deep ocean temperature variability.

Both Waelbroeck et al. (2002) and Cutler et al. (2003) found significant differences in deep ocean temperature variability between ocean basins, with typical last glacial to interglacial deep temperature warming reaching 3–4 °C in the South Indian and Atlantic Ocean and 2 °C in the Pacific Ocean. In both the Atlantic and South Indian Ocean basins Waelbroeck et al. (2002) found that deep ocean temperatures fluctuated on precessional, obliquity and millennial time scales during at least the last four glacial cycles. Millennial scale temperature variability in the deep North Atlantic is supported by Mg/Ca temperature estimates (Skinner and Elderfield, 2007). However, both Waelbroeck et al. (2002) and Cutler et al. (2003) find that deep Pacific temperatures did not vary significantly during the last glacial period (i.e. Marine Isotope Stages (MIS) 4, 3 and 2), and in agreement with the results of Chappell and Shackleton (1986), find that the deep Pacific warmed by ~2 °C between the last glacial maximum (LGM) and the Holocene.

Duplessy et al. (2002) calculated deep ocean temperatures at the LGM relative to the Holocene. These authors assumed that the change in benthic oxgen isotopes due to the loss of the continental ice sheets since the LGM was 1.05 ± 0.20‰ (Adkins and Schrag, 2001). By removing this value from Holocene $\delta^{18}O_b$ measurements these authors were able to calculate the proportion of the benthic isotope record that could be explained by local temperature variations using the Shackleton (1974) temperature equation. Duplessy et al. (2002) concluded that the deep Pacific was at least 1.3 °C above freezing point at the LGM.

Modeling methods for inferring sea-level records from benthic oxygen-isotope records have also been used. For example, Bintanja et al. (2005) and Bintanja and van de Wal (2008) used an ice-sheet model coupled to a model of benthic isotope fractionation to derive both sea level and high-latitude temperature with some success. Based on climate-model results, these authors assumed a constant link between high latitude temperature and deep ocean temperature. Consequently, this work does not allow for the possibility that the deep ocean temperature varies between ocean basins or has a time–variable relationship between the surface and deep. Instead, these authors take only tentative steps to reconcile their method with the issue of hydrographic variations in benthic oxygen-isotope records between ocean basins by using a stacked benthic isotope record (Lisiecki and Raymo, 2005) and carrying out sensitivity tests with a series of benthic isotope records from different ocean basins.

1.3. Other deep ocean temperature proxies

In addition to the use of benthic oxygen isotope ratios to derive deep ocean temperature as discussed above, two other methods to derive benthic temperature require note. Adkins et al. (2002) measured oxygen isotope ratios in sediment pore waters from the LGM. By comparing the change in pore water oxygen isotope ratios with the oxygen isotope ratios in benthic foraminifers these authors were able to calculate deep ocean temperatures at the LGM. They concluded that bottom water masses were close to freezing at the LGM in much of the deep ocean. Although this result applies uniquely to the LGM, the work of Chappell and Shackleton (1986), Waelbroeck et al. (2002) and Cutler et al. (2003) suggest that the deep Pacific was close to the freezing point through an extended period during the last glacial cycle.

Mg/Ca ratios on benthic foraminifers have been used to estimate temperature variability in the equatorial Pacific during the last glacial cycle (Martin et al., 2002). These authors estimate the glacial to interglacial deep Pacific to warm by 2–3 °C, in agreement with estimates based on oxygen isotope ratios in benthic foraminifers and sediment pore water oxygen isotope ratios. However, the Mg/Ca record of Martin et al. (2002) implies temperature variability in

the deep Pacific of approximately half a degree during the glacial period, whereas temperatures calculated from benthic oxygen-isotope records indicate little or no variability. Martin et al. (2002) note that the relationship between Mg/Ca and temperature is particularly sensitive at the low temperatures during the glacial and that the core-top dataset used to calibrate the Mg/Ca data was limited. Skinner and Shackleton (2005) reconsider the Martin et al. (2002) Mg/Ca dataset in some detail and suggested that species specific sensitivities might make this dataset unreliable. In addition, Elderfield et al. (1996) suggest that benthic Mg/Ca temperature estimates are compromised by varying deep-sea carbonate-ion concentrations, where benthic Mg/Ca decreases with ΔCO_3^{2-} (see also Yu and Elderfield (2008)).

Whichever reconstruction one chooses, there appears a decoupling of the benthic temperature and sea-level reconstructions in the deep Pacific during glacial periods. That is, deep Pacific temperature variability is below the detection limit of existing methods while sea-level appears to have undergone substantial changes. Here we explore when this decoupling between temperature and sea level began and its implications for glacial variability.

2. Data and methods

For the sake of simplicity, we follow an approach similar to that of earlier studies (Chappell and Shackleton, 1986; Waelbroeck et al., 2002; Cutler et al., 2003). As described, this involves scaling benthic oxygen isotope ratios to sea level using a series of independent sea-level markers. We extend the period of analysis to the last 5 Myr. In this section we define the benthic oxygen-isotope record, sea-level markers, and methodology we use for the calculation of sea level and deep ocean temperature.

We follow a number of previously published studies in making the assumption that the benthic oxygen-isotope record is, after factoring out temperature, indicative of global changes the oxygen isotope content of the water (Chappell and Shackleton, 1986; Waelbroeck et al., 2002). The deep Pacific is composed of waters originating across the world's oceans, and a change in end member characteristics or the ratio of contribution between end members will also influence local values of the oxygen isotope content of the water. Thus, regional variations in hydrography will introduce uncertainties in our sea level reconstruction, though the shear size of the Pacific basin, if considered in aggregate, does help insure that this basin will not differ greatly from the global mean.

2.1. Data

The last two glacial cycles span the best understood period of sea-level variability and most of our sea-level markers derive from this period. We also include sea-level estimates for the mid-Pliocene. These sea-level estimates and the periods to which they correspond are listed in Table 1. We use the composite deep Pacific benthic oxygen-isotope record published by Shackleton et al. (1990), which comprises cores V19-30 (3° 23′ S, 83° 31′ W, 3091 m), ODP 677 (1° 12′ N, 83° 44′ W, 3450 m) and ODP 846 (3° 5.7′S, 90° 49.1′ W, 3296 m) (Fig. 1A). For each period listed in Table 1 we take the mean oxygen isotope ratio from the composite deep Pacific benthic isotope record and an estimate of the sea-level.

Sea level estimates and their uncertainties come from ice-sheet volume and relative sea level constraints. Where we use benchmark sea-level indicators such as fossil coral reefs or submerged speleothem records, we only discuss sites distant from the former ice sheet margins, which can be considered to represent eustatic sea level to within several (i.e. typically < 2–3) meters (Bassett

Table 1
The sea-level constraints for specific periods in the composite benthic oxygen-isotope record of Shackleton et al. (1990). Details are given in the text. The uncertainty in the oxygen isotope ratios is based on the standard deviation of Holocene observations except the mid-Pliocene value, which is based on the standard deviation during this period.

Period	Sea level	Reference	Ages	$\delta^{18}O_b$ (VPDB)
Mid-Pliocene	+28 ± 16 m	1	4–5 Ma BP	2.6 ± 0.2
MIS 7e	−10 ± 5 m	2	236–238 ka BP	3.8 ± 0.1
MIS 7c	−12.5 ± 2.5 m	2	206.5–216.5 ka BP	3.8 ± 0.1
MIS 7a	−12.5 ± 2.5 m	2	194–200 ka BP	3.9 ± 0.1
MIS 5e	+4.5 ± 1.5 m	3	116–124 ka BP	3.4 ± 0.1
MIS 5c	−15.5 ± 1.5 m	4	94–105 ka BP	4.1 ± 0.1
MIS 5a	−15.5 ± 1.5 m	4	77.5–85 ka BP	4.1 ± 0.1
MIS 4	−90 ± 10 m	5	62–68 ka BP	4.6 ± 0.1
MIS 3	−70 ± 20 m	6	35–60.5 ka BP	4.5 ± 0.1
MIS 2 (LGM)	−130 ± 10 m	7	17–20 ka BP	5.0 ± 0.1
MIS 1 (Holocene)	0 m	–	0–7 ka BP	3.5 ± 0.1

1. Bamber et al. (2001), Lythe et al. (2001), Oerlemans and Van der Veen (1984).
2. Bard et al. (2002), Antonioli et al. (2004), Siddall et al. (2003).
3. Stirling et al. (1998), Thompson and Goldstein (2006), Antonioli et al. (2007).
4. Schellmann and Radtke (2004).
5. Bard et al. (1990), Cutler et al. (2003), Siddall et al. (2003).
6. Siddall et al. (2003), Siddall et al. (2008), Chappell (2002).
7. Fairbanks (1989), Yokoyama et al. (2000).

et al., 2005). Note that there is inadequate data and understanding of isostatic processes during this interval to be more exact. There is some evidence for variability of several (i.e. of the order of 2–3 m) within a given Marine Isotope Stage (Thompson and Goldstein, 2005, 2006; Rohling et al., 2008), commensurate with our uncertainty estimates. For a more detailed discussion of sea level we refer the reader to the review of interglacial sea level during the last million years by Siddall et al. (2006).

2.1.1. The mid-Pliocene

There is considerable disagreement between sea-level reconstructions for the mid-Pliocene. Published estimates range from 5 m above modern sea level (Miller et al., 2005) to 44 m above modern sea level (Oerlemans and Van der Veen, 1984). We consider two alternative scenarios for possible changes to global ice volume during the mid-Pliocene. Evidence for the lack of a Greenland ice sheet (GIS) during this period comes from the modeling work of Lunt et al. (2008). In the absence of a GIS, sea level would have been 7 m higher than today (Bamber et al., 2001). We assume that the West Antarctic ice sheet (WAIS), which currently sits below modern sea level (Lythe et al., 2001), would not be stable at a sea level 7 m higher than today. We therefore allow for the additional WAIS contribution of 5 m to global sea level (Lythe et al., 2001). GIS and WAIS contributions would give a sea level of 12 m above present. Therefore, as a lower estimate on the height of eustatic sea-level during this period, we assume the GIS and WAIS were not present but that the East Antarctic ice sheet (EAIS) was in its modern configuration. As an upper estimate we take the results of Oerlemans and Van der Veen (1984) who found that the EAIS was reduced to 1/3 of its modern extent during this period, giving a high sea level of 44 m above modern levels. Because we focus on changes during the mid-Pleistocene Transition our conclusions are not sensitive to the choice of sea level to the wide range of values we consider for the sea level during the mid-Pliocene.

2.1.2. MIS 7a,c,e

Sea level during MIS 7 has been a subject of some disagreement. Evidence from U/Th dated fossil coral reefs from Hawaii points to sea level close to or slightly below modern (Gallup et al.,
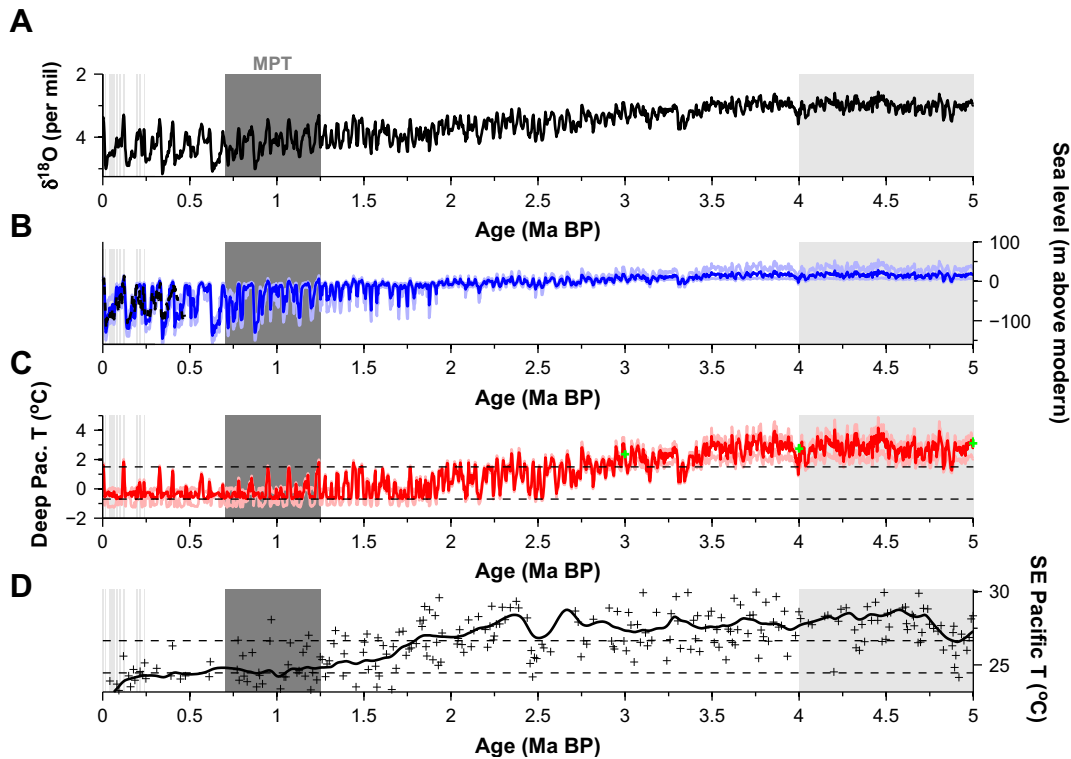
Fig. 1. A) The composite oxygen-isotope record of benthic foraminifers for the deep Pacific on the astronomical time scale published by Shackleton et al. (1990) comprising cores V19-30, ODP 677 and ODP 846. B) The sea-level record calculated by linear interpolation of independent sea-level markers listed in Table 1 (blue line) and calculated uncertainty (light blue lines). The light grey bars indicate the periods in the oxygen-isotope record for which mean oxygen isotope data and standard deviations are taken to construct the calibration shown in Fig. 2. The black dashed line shows the sea level reconstruction based on Red Sea core MD921017 (Siddall et al., 2003). C) The temperature residual represents the component of the benthic oxygen-isotope record which cannot be explained by sea level. We scaled the residual to temperature using the Shackleton (1974) temperature equation (red lines, Equ. (3)) and calculated an uncertainty interval (pink lines). See text for further explanation. The dark grey bar represents the MPT. The green crosses and vertical lines are the Mg/Ca temperature estimates from the deep Pacific allowing for the uncertainty due to variations in the carbonate-ion concentration in the deep Pacific (Lear, 2007). D) The Mg/Ca surface temperature reconstruction from the SE Pacific of Wara et al. (2005) (crosses) and the same data with a 0.2 Ma Butterworth filter. Dashed lines indicate a 2 °C interval to indicate that the cooling at the surface and the deep ocean were both coincident and of a similar magnitude.

1994). Contrastingly, evidence from the Argenterola Cave submerged speleothem record points to sea level between −15 and −10 m below modern for MIS 7a and 7c, and sea level between −15 and −5 m for MIS 7e (Bard et al., 2002; Antonioli et al., 2004). Independent estimates of sea level during this period are given by Siddall et al. (2003) based on a model of the sensitivity of the Red Sea oxygen-isotope record on planktic foraminifers to sea level change. The sea-level estimate from these authors is between −15 and −10 m, in good agreement with the estimates from Argenterola Cave. This agreement leads us to assume values of between −15 and −10 m below modern for MIS 7a and 7c, and sea level between −15 and −5 m for MIS 7e. For each of the substages we take the midpoint of each of these ranges as our best estimate.

2.1.3. MIS 5e

Sea-level for MIS 5e is taken from relatively stable sites distant from the large continental ice sheets. Relative sea level high stands during MIS 5e vary from 3 m above modern for sites in Western Australia (Stirling et al., 1998) to 6 m above modern in the Bahamas (Thompson and Goldstein, 2006) and 5 m above modern in the Mediterranean (Antonioli et al., 2007). Regional variations in relative sea level are due in part to the visco-elastic isostatic responses of the earth's crust, which lag the collapse of the ice sheets and have a significant regional imprint. To allow for uncertainties in correcting these effects we simply take the range and midpoint of observed relative sea level, yielding an MIS 5e eustatic sea level of 4.5 ± 1.5 m.

2.1.4. MIS 5a,c

Sea level during MIS 5a and 5c is suggested by the relative vertical positions of uplifted fossil coral terraces on Barbados formed during these substages relative to the MIS 5e high stand (Schellmann and Radtke, 2004). These terraces are found 20 m below the MIS 5e terrace indicating that sea level was 15.5 ± 1.5 m below modern during this period (i.e. 20 m below the sea level for the MIS 5e high stand).

2.1.5. MIS 4

Independent evidence for the extent of the MIS 4 sea-level low stand comes from fossil coral evidence from Barbados, which indicates that sea level was 81 ± 5 m below present at the start of MIS 4 (Bard et al., 1990; Cutler et al., 2003). The Red Sea sea-level technique gives an estimate of 100 m below modern (Siddall et al., 2003). Given this range of estimates we take a value of 90 ± 10 m as representative of sea level during MIS 4.

2.1.6. MIS 3

Chappell (2002), Yokoyama et al. (2001) and Siddall et al. (2003) among others have all presented evidence of millennial scale sea-level fluctuations during MIS 3 on the order of 10–30 m in magnitude. Recently, Siddall et al. (2008a) published a review of evidence for sea-level change during MIS 3 and concluded that MIS 3 sea level varied around a mean value of 70 m below modern sea level, which we take as the best estimate with an upper and lower limit of 50 and 90 m below modern sea level to allow for uncertainty and variations during this interval.

2.1.7. LGM

Estimates for LGM (∼20 ka BP) sea level vary between 120 m below modern sea level based on Barbados fossil coral reef evidence (Fairbanks, 1989) and 140 m below modern sea level based on sedimentary sequences from Bonaparte Gulf (Yokoyama et al., 2000). Note that the Bonaparte Gulf estimate has been corrected for local isostatic effects (Yokoyama et al., 2000) but the Barbados estimate has not (Fairbanks, 1989). Peltier and Fairbanks (2006) argue that Barbados is positioned so as not to need significant isostatic correction. We assume a best estimate of 130 ± 10 m below sea level to allow for this range of estimates.

2.2. Sea-level calibrations

Fig. 2 shows the scaling of the benthic oxygen-isotope record to sea level. Each point represents the sea-level data shown in Table 1 and the mean benthic oxygen isotope value for the corresponding period, as shown in Fig. 1. An uncertainty of 0.1‰ in the oxygen isotope ratios is based on the standard deviation of Holocene observations, except for the mid-Pliocene, where 0.2‰ is more representative of the uncertainty. As noted above, we assume that the sea-level data shown in the figure correspond to a representative value through each period. This calibration provides a non-linear transfer function by which to convert the benthic isotope data to sea level, and which we will refer to as the sea level transfer function. Note that we use a piece-wise linear approach to estimating the sea level transfer function, applying a simple linear interpolation of the benthic isotope values between sea-level markers.

Because our calibration is focused on individual marine isotope stages our method is limited to consideration of orbital time scales. Waelbroeck et al. (2002) considered a high resolution dataset of U/

Th dated sea-level markers during the Last Glacial Cycle and found a hysteresis behaviour in the relationship between benthic oxygen isotopes and sea level. This hysteresis differentiates the relationship between benthic oxygen isotopes and sea level during glacial inception and termination and is due to the difference in mean ice-sheet response, which is slightly slower during inceptions compared to terminations (e.g. Bintanja and van de Wal, 2008; Siddall et al. 2008b). In addition, millennial variability influences deep-sea temperature and ice volume at different times during glacial terminations, indicating that millennial sea-level variability is at best poorly resolved by benthic oxygen isotope measurements during terminations (Skinner and Shackleton, 2005; Skinner and Elderfield, 2007). These effects occur on time scales of several millennia and are not resolved by our method.

In constructing this transfer function we have made two major assumptions. First, as discussed, that the composite $\delta^{18}O_b$ is representative of the average oceanic conditions. Second, that the relation between $\delta^{18}O_b$ and sea level is approximately constant throughout the Pleistocene, which is almost certainly not the case given the likelihood of local variations. One major source of uncertainty is that the mean $\delta^{18}O$ of the ice locked up in ice sheets can change independent of their volume. For example, a fully developed Laurentide ice sheet might be expected to cause greater fractionation in the precipitation which maintains it, but which would only gradually replace the less fractionated precipitation involved in the initial growth of the ice sheet. Because the $\delta^{18}O$ in accumulated ice would differ from the $\delta^{18}O$ in ablated ice (which is observed in the ocean), benthic oxygen isotopes could become decoupled from either temperature or ice volume. Further, thermal expansion of the ocean is not considered in these calculations, nor regional changes in temperature, but which could explain some 0.2–0.6 m °C^{-1} of sea-level rise (Meehl et al., 2007). These additional complications merit further study, but we proceed with the current analysis assuming a constant $\delta^{18}O_b$ – sea level relationship in order to first map out the implications of the simpler scenario.

Some reassurance that the sea-level transfer function is at least plausible is given by the fact that our empirical approach provides a monotonically increasing relationship between the benthic oxygen isotope data and sea level, as might be expected (see Fig. 2). Two theoretical constraints on the sea-level transfer function are provided by the freezing point of seawater (−1.7 °C in the deep eastern equatorial Pacific (Duplessy et al., 2002)) and the disappearance of major continental ice masses. Thus, two asymptotes should exist, one nearly vertical (along an isotherm) and one more horizontal at the level of 'near zero land ice' where sea level is uniquely sensitive to thermal expansion. Although the major continental ice masses do not disappear in the time-frame of this study, one may expect a reduction in the sensitivity of the benthic oxygen isotopes to sea-level change at warmer temperatures. Given these theoretical constraints, the shape of the transfer function shown in Fig. 2 appears reasonable.

Lines of equal temperature (isotherms) are shown in Fig. 2. If the calibration curve follows these isotherms it implies that all of the benthic oxygen-isotope record can be explained by ice-volume change. In contrast, calibration curves crossing isotherms imply that sea-level and temperature changes both contribute to the benthic oxygen isotope variations. One implication of the transfer function is that $\delta^{18}O_b$ is less sensitive to global temperature and sea level during times of high sea level, at least during the Plio-Pleistocene.

2.3. Calculation of temperature

We use the sea level transfer function to partition the $\delta^{18}O_b$ record into sea level and temperature components as follows:
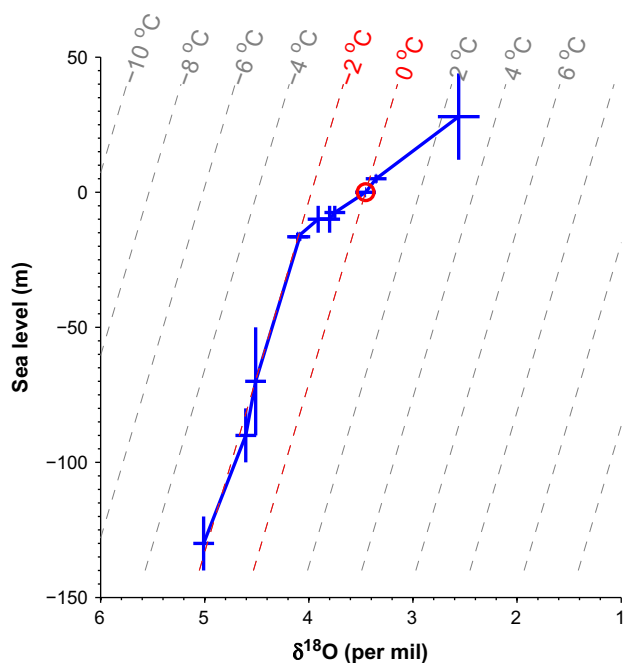

Fig. 2. The sea-level markers listed in Table 1 plotted against the mean benthic oxygen isotope values and standard deviations for the periods shown by the grey bars in Fig. 1 and listed in Table 1. The red circle indicates late Holocene values. The diagonal dashed lines indicate isotherms relative to the mean Holocene value for the last 7 kyr. When the sea-level calibration runs parallel to these lines 100% of the benthic oxygen isotope signal can be explained by sea-level variation. Isotherms are shown relative to Holocene values and represent the global mean sea-level slope (1.1‰ for 130 m of sea-level change) separated by 2 °C, as calculated by rearranging Equ. (3) (Shackleton, 1974).

1. Estimate sea level (SL$_b$) by processing the δ^{18}O$_b$ using the transfer function derived above.
2. Obtain the global mean change in the oxygen-isotope record due to the growth of the major ice sheets (δ^{18}O$_w$) by multiplying (SL$_b$) by a scaling factor based on LGM data,

$$\delta^{18}O_w = \frac{\Delta\delta^{18}O_{present-glacial}}{\Delta SL_{LGM}} \cdot SL_b. \qquad (1)$$

The scaling factor is defined as the global mean change in oxygen isotope ratios between the present and LGM, $\Delta\delta^{18}O_{present-glacial}$, divided by the sea level change between the present and LGM, ΔSL_{LGM}. We use the estimates provided by the study of oxygen isotope ratios in sediment pore water from the LGM of Adkins et al. (2002). LGM to Holocene variation in oxygen isotope ratios in water, as measured on pore waters in marine sediment cores, suggests some degree of spatial heterogeneity between ocean basins of between 0.7 ± 0.1‰ in the North Atlantic and 1.3 ± 0.2‰ in the Southern Ocean (Adkins et al., 2002). These differences can be explained by changes in deep ocean hydrography since the LGM in these basins. Following previous studies (Chappell and Shackleton, 1986; Waelbroeck et al., 2002; Cutler et al., 2003) we assume a constant value for $\Delta\delta^{18}O_{present-glacial}$ of 1.1 ± 0.1‰ based on deep Pacific values (Adkins et al., 2002) and a value for SL$_{LGM}$ of 130 ± 10 m (see section 2.1.7). To check the accuracy of this approximation we will compare our temperature reconstructions with independent estimates of temperature in Section 4.4.

3. Having estimated the ice volume component of the benthic oxygen-isotope record, it can now be subtracted from the original benthic isotope record (δ^{18}O$_b$), yielding a residual which we interpret as the component of the benthic isotope record related to variations in temperature,

$$\delta^{18}O_t = \delta^{18}O_b - \delta^{18}O_w. \qquad (2)$$

4. The δ^{18}O$_t$ residual is converted to temperature using the Shackleton (1974) temperature scaling,

$$T = 16.9 - 4.38 \cdot \delta^{18}O_t + 0.1 \cdot \delta^{18}O_t^2 \qquad (3)$$

3. Results

3.1. Changes over the last 5 Ma

Fig. 1 shows the time series of the benthic oxygen isotope compilation of Shackleton et al. (1990) (Fig. 1A), the sea-level record following the scaling shown in Fig. 2 (Fig. 1B), and the temperature residual calculated according to the procedure outlined in Section 2.3 (Fig. 1C).

We first note that our scaling implies that deep ocean temperature varied by approximately 2 ± 1 °C at glacial/interglacial time scales during the last 5 Ma (Fig. 1C). The amplitude of the temperature variability stays nearly uniform over time, unlike the benthic oxygen-isotope record (Fig. 3A,C) (Clark et al., 2007; Huybers, 2007; Lisiecki and Raymo, 2007). The amplitude of ice volume variability, however, increases dramatically from the order of tens of meters to hundreds of meters (Fig. 3B).
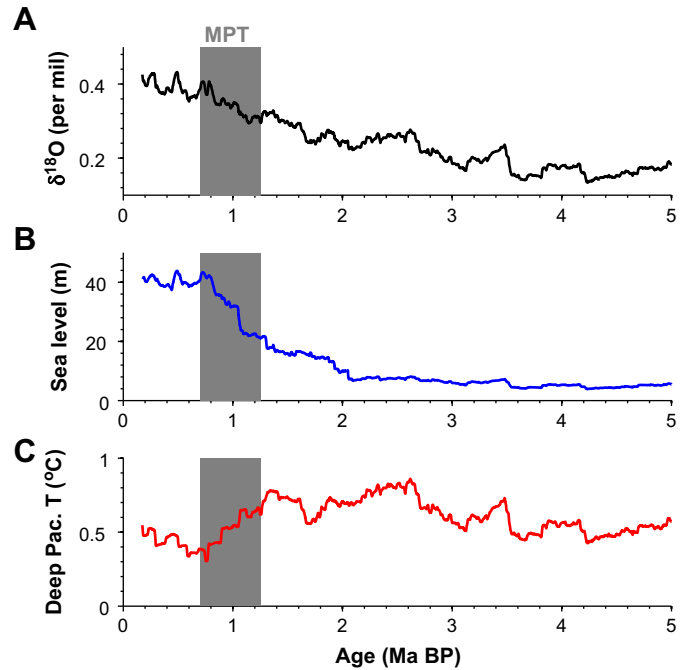

Fig. 3. The standard deviation of the records using a 350 kyr sliding window with a 349 kyr overlap (i.e. the standard deviation is taken for 350 kyr intervals, each separated by 1 kyr). A) δ^{18}O$_b$ for the deep Pacific. B) Sea-level C) Bottom water temperature for the deep Pacific. The dark grey bars and lines represent the MPT.

Prior to the MPT our scaling implies that Pacific deep ocean temperature and ice volume varied in concert (Figs.1B,C and 2). Cooling in the deep Pacific is associated with ice sheet growth and a warming in the deep Pacific is associated with ice sheet collapse, albeit with the inertia associated with ice sheets causing this component to lag. During the MPT temperature and ice volume begin to decouple. Deep ocean temperature continues to cool until the last 2 Ma when the glacial minima begin to asymptote towards freezing conditions in the deep ocean, while glacial ice volume maxima continue to increase. Further cooling is not possible but the duration of the periods with cold, stable conditions continue to extend. This process continues until the MPT is complete and the interglacial periods are the only periods when the deep Pacific temperature breaks away from the relatively constant values (i.e. below the detection limit of our method, which is ± 1 °C) of the glacial periods. The deep Pacific temperature record takes on the character of relatively sharp interglacial pulses with a $\sim$100 kyr period (Fig. 1C).

During the last 700 kyr, much of the interglacial minima in the oxygen-isotope record can be explained as resulting from temperature changes. This can be seen in Fig. 1C, which shows the temperature residual from our sea-level scaling. The temperature residuals show a clear $\sim$100-kyr pulse, similar to previous studies (Chappell and Shackleton, 1986; Waelbroeck et al., 2002; Cutler et al., 2003). Bintanja et al. (2005) and Bintanja and van de Wal (2008) found a glacial to interglacial temperature range of 2–3 °C, in agreement with these results, but their cooling trend into the glacial period occurred much more gradually.

Note that although our sea-level reconstruction is similar to those of Bintanja et al. (2005) and Bintanja and van de Wal (2008), direct comparison of the Bintanja et al. deep-sea temperature reconstructions and our temperature reconstruction is inappropriate because we only consider the deep Pacific temperature while Bintanja et al. considered a globally stacked record.

3.2. Spectral analysis over the last 5 Ma

Fig. 4 shows the spectrogram for the temperature and sea-level components of the composite benthic oxygen-isotope record from the deep Pacific and the temperature and sea-level records calculated in this paper. To precondition the record for evolutive spectral analysis, the long-term trend was removed from these records using a 350 kyr high-pass butterworth filter. Note that the change in power as time progresses for the temperature reconstruction (the plots show relatively similar amounts of red and blue for early periods as later periods, Figs. 3C and 4C) is less than that for the sea-level reconstruction (the plot is more blue for the early period and becomes red as the ∼100 kyr glacial cycles commence, Figs. 3B and

4B). Indeed, the glacial to interglacial range in deep ocean temperature varies little during the last 5 Ma (Fig. 3C). This is not the case for sea level, which varied little during the mid-Pliocene (4–5 Ma BP) but began to vary increasingly during the MPT (Figs. 4B and 3B). By combining these two effects, $\delta^{18}O_b$ represents an intermediate signal with some increase in power over the MPT (Fig. 4A).

In order to consider the relative switch in the power in the 100-kyr range from the 41-kyr band, we normalize the spectral power estimate in each band of the spectrum by the power concentrated just in the 41-kyr obliquity band,
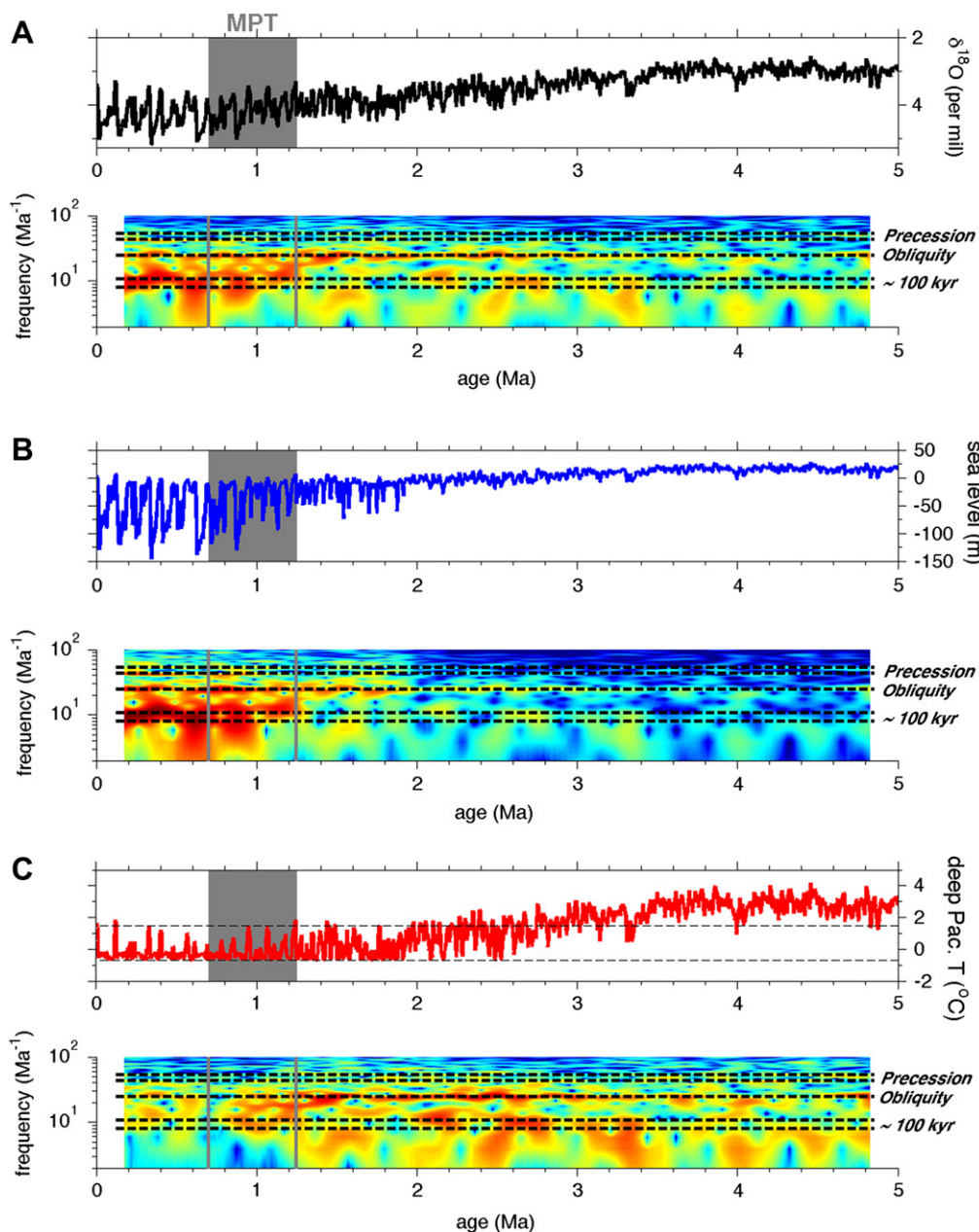
$$R = P/P_{obliquity} \tag{4}$$

Fig. 4. A) Time series of $\delta^{18}O_b$ for the composite record from the deep Pacific of Shackleton et al. (1990) (upper panel). Corresponding spectrogram for the same record (lower panel). B) Time series of sea-level calculated from the composite $\delta^{18}O_b$ for the deep Pacific (upper panel). Corresponding spectrogram for the same record (lower panel). C) Time series of bottom water temperature calculated from the composite $\delta^{18}O_b$ for the deep Pacific (upper panel). Corresponding spectrogram for the same record (lower panel). To facilitate spectral analysis the records were first filtered with a 350-kyr Butterworth filter in both forward and backward directions to avoid any phase distortion. The spectrograms shown here represent Fourier transforms with a 350-kyr window with a 349-kyr overlap. The dark grey bars and lines represent the MPT.

Fig. 5 shows R_δ, R_T and R_{SL} where the subscripts δ, T and SL represent $\delta^{18}O_b$, temperature and sea level, respectively. R values greater than 1 indicate that more power may be found in that part of the spectrum compared to the obliquity band. Prior to the MPT the relative spectra evolve in a very similar fashion for $\delta^{18}O_b$, sea level and temperature. However, through the MPT and beyond, the sea level and deep ocean temperature become increasingly distinct (Fig. 5B,C).

The 100-kyr 'pulse' in deep-sea temperature does not strongly register in the Fourier transform shown in Fig. 3C or Fig. 5C. Instead, most of the power remains restricted to the obliquity band, suggesting that the '100 kyr' pulses in deep water temperature are in fact multiples of the obliquity band signal (i.e. 41, 82 and 123 kyr). Indeed, Huybers and Wunsch (2005) and Huybers (2007) suggest that the ~100 kyr variability in the benthic isotope record is in fact generated by the 'skipping' of obliquity cycles. This finding is consistent with the findings of Bintanja and van de Wal (2008).

4. Discussion

4.1. Implications for the analysis of benthic oxygen-isotope records

Perhaps the first lesson that one appreciates from this exercise is that the spectra of the deep-sea temperature and sea level
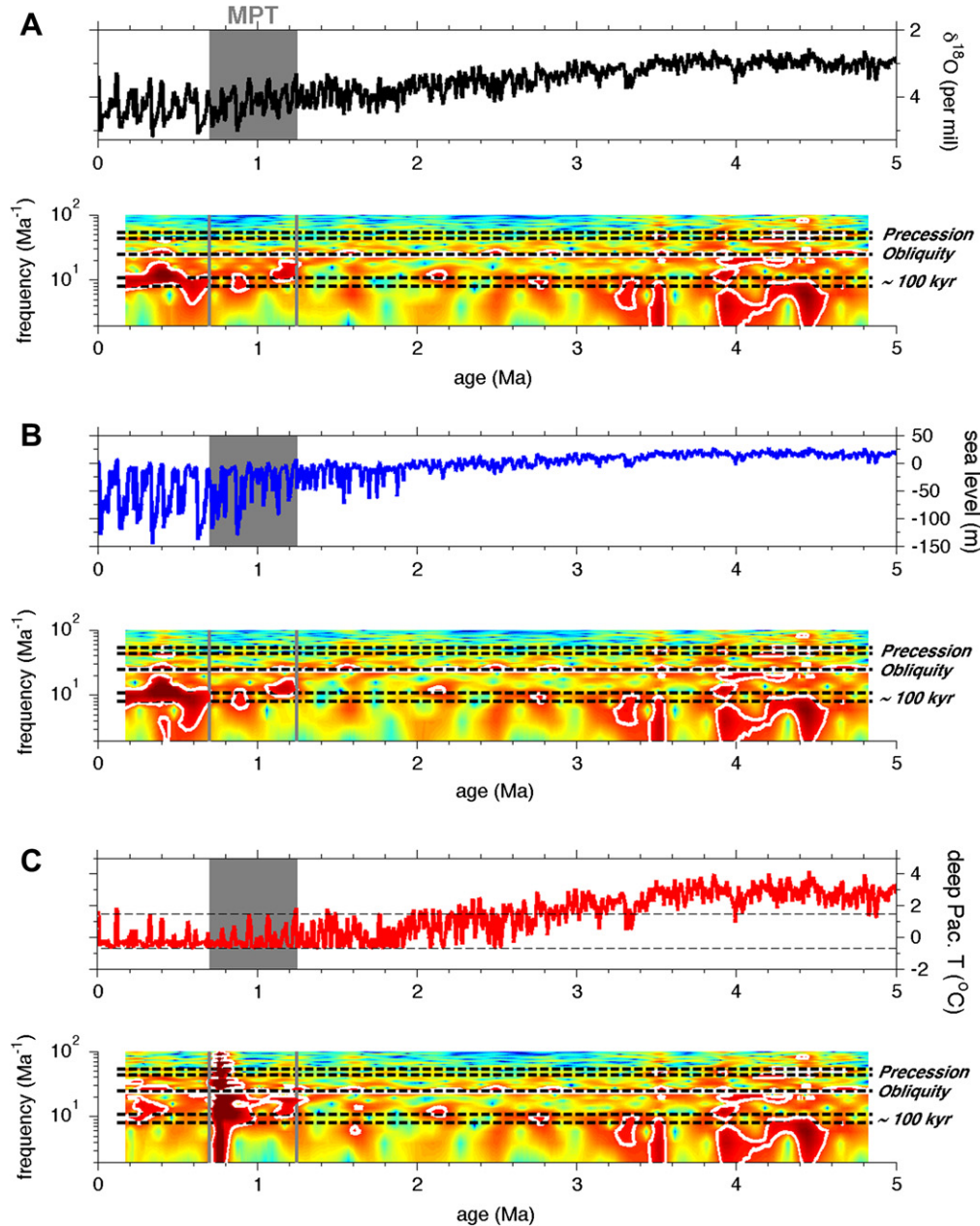

Fig. 5. A) Time series of $\delta^{18}O_b$ for the composite record from the deep Pacific of Shackleton et al. (1990) (upper panel). R_δ for the same record (lower panel). B) Time series of sea-level calculated from the composite $\delta^{18}O_b$ for the deep Pacific (upper panel). R_{SL} for the same record (lower panel). C) Time series of benthic temperature calculated from the composite $\delta^{18}O_b$ for the deep Pacific (upper panel). R_T for the same record (lower panel). To facilitate spectral analysis the records were first filtered with a 350-kyr Butterworth filter in both forward and backward directions to avoid any phase distortion. The spectrograms shown here represent Fourier transforms with a 350-kyr window with a 349-kyr overlap. R values are the power spectra normalised to the power in the obliquity band after Equ. (4) (see text for details). White contours represent $R = 1$, where the power at a given frequency is equal to that in the obliquity band. The dark grey bars and lines represent the MPT.

components of the benthic oxygen-isotope record are distinctly different during the last 700 kyr. If one was to assume that the spectral analysis of the benthic oxygen-isotope record for the last 700 kyr was equivalent to the spectra of continental ice volume (e.g. Clark et al. (2006), Huybers (2007), Lisiecki and Raymo (2007) and many others) one would mistakenly assume that the spectra in deep ocean temperature and sea level are equivalent. In fact, the spectra of deep ocean temperature and sea level are not equivalent. In particular, our results indicate that deep ocean temperature represents a pulse of warming on the 100-kyr time scale. The Fourier transforms shown in Figs. 4C and 5C indicate that this apparent 100-kyr signal is in fact dominated by power in the obliquity band and these results support the assertion of Huybers and Wunsch (2005) and Huybers (2007) that the 100-kyr signal is made up of multiple obliquity cycles.

It is striking that deep Pacific temperature records maintain an amplitude of 2 °C over the last 5 Ma, while the variability in ice volume increases from several to around 100 m. The increase in the variance of the Pacific benthic oxygen-isotope records over the last several Ma (Clark et al., 2007; Huybers, 2007; Lisiecki and Raymo, 2007) can therefore be explained by the ice volume component, rather than the temperature component, presumably because ice volume becomes increasingly sensitive to temperature change at lower temperatures. The reduced sensitivity of ice volume to temperature at warmer temperatures can be seen in Fig. 6, which compares the sea-level indicators listed in Table 1 with the temperature record for the deep Pacific derived here and temperatures derived from the EPICA Dome C ice core record
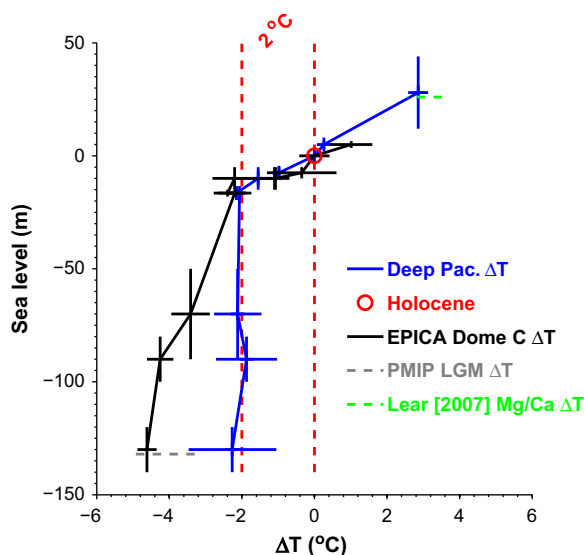

Fig. 6. An illustrative plot of the sensitivity of global ice volume (sea level) to temperature change across different temperature indicators: deep Pacific temperature (blue) derived here from the $\delta^{18}O_b$ compilation from the deep Pacific of Shackleton et al. (1990) and temperature derived from the EPICA Dome C ice core (black) (Jouzel et al., 2007) (allowing for a polar amplification factor of 2 (Hansen et al., 2007), note this is only used here as an approximate indicator). Also shown is the PMIP 2 global mean temperature reconstruction for the last glacial maximum (LGM) from a range of global climate models (grey dashed line, position on *y*-axis is just for illustration) (Jansen et al., 2007). The dashed green line represents the range of Mg/Ca temperature estimates from the deep Pacific between 5 and 4 Ma (Lear, 2007). This allows for uncertainty due to the carbonate ion effect by taking the maximum and minimum values estimates 5 and 4 Ma (see also Fig. 1C). Temperature reconstructions are given relative to Holocene mean (last 7 kyr). Mean temperatures and standard deviations are for the periods shown by the grey bars in Fig. 1 and listed in Table 1. Sea-level indicators and uncertainties for different Oxygen Isotope Stages, as in Fig. 2. Note that temperature in the deep Pacific did not vary during the glacial period (MIS 4–MIS 2). In this figure this is shown by the ~2 °C cooling between the Holocene and glacial period indicated by the dashed red line.

published by Jouzel et al. (2007), the Paleoclimate Model Intercomparison Project 2 (Jansen et al., 2007) and Mg/Ca temperature estimates for the deep Pacific from the mid-Pliocene (Lear, 2007). We include EPICA temperatures in this illustrative comparison because, unlike deep Pacific temperatures, these vary during the glacial period and give an indication of the relationship between global ice volume and temperature during the glacial period.

There is another important point to note for the interpretation of ice volume from benthic oxygen-isotope records. If one were to assume a direct link between deep Pacific temperature and high-latitude atmospheric temperature, one would risk making systematic errors because deep Pacific temperature does not in fact vary during recent glacial periods. During interglacial periods our study suggests a linear relationship between deep Pacific temperature and sea surface temperature, but that this breaks down during the glacial period. Bintanja et al. (2005) and Bintanja and van de Wal (2008) applied the benthic oxygen isotope stack of Lisiecki and Raymo (2005) in their model rather than an oxygen-isotope record derived uniquely from the deep Pacific (as is the record we use here), thereby avoiding this problem. Nevertheless, our results are important for those interested in carrying out similar studies in the future.

4.2. Speculation as to why the deep Pacific temperature may respond in this way

Chappell and Shackleton (1986) assumed that deep Pacific temperatures varied little during recent glacial periods because they approached freezing point. However, the work of Waelbroeck et al. (2002) indicates that the deep Pacific temperature might have remained around 0 °C, that is above freezing point of the deep ocean. An alternative mechanism is a reduced contribution of North Atlantic Deep Water (NADW) to the Circumpolar Deep Water (CDW). At present, NADW provides a source of relatively warm, salty water to the Southern Ocean. Therefore, changes in the strength and properties of NADW formation may affect the temperature and salinity of CDW and the Pacific. We speculate that the shoaling of NADW during the glacial period (e.g. Curry and Oppo, 2005) reduced its influence on CDW and thereby muted the variability otherwise associated with changes in NADW properties. The shoaling of NADW would explain why Waelbroeck et al. (2002) found important temperature influences on the benthic oxygen-isotope records from the North Atlantic and South Indian Ocean but not in the deep Pacific.

4.3. Implications for 100-kyr variability

The existence of a strong 100-kyr 'pulse' in the deep Pacific temperature over the last 700 kyr may point to the non-linearity in the deep Pacific temperature as a fundamental aspect in governing the 100-kyr variability. That this non-linearity came about during the MPT, when the pacing of glacial cycles changed from the 41-kyr to 100-kyr periodicity, supports this inference. Here we discuss the possible links between deep Pacific temperature and the glacial cycles.

We first consider changes in the Southern Ocean. It stands to reason that changes in the Southern Ocean, where much of the waters filling the Pacific originate from, will then also influence the deep Pacific. A recent modeling study similarly concluded that Southern Ocean processes may be key to understanding the 100-kyr variability but did not specify what these processes may be (see Köhler and Bintanja (2008) and references therein). Changes in the Southern Ocean have a direct impact on the sequestration of CO_2 in the deep ocean. Monnin et al. (2001) suggest that changes in glacial CO_2 storage in the deep ocean are only linked to a fraction of the

glacial to interglacial CO_2 change, though other changes related to circulation or biological activity could also become important. Even if that is the case, processes in the deep Pacific may still explain the 100-kyr variability in CO_2 by initiating positive feedbacks with other mechanisms on the 100-kyr time scale. Our results then are in broad agreement with the findings of Shackleton (2000) who concluded that deep Pacific temperature follows a spectral pattern similar to that of atmospheric CO_2 concentrations (with a strong emphasis on 100-kyr variability) but a different pattern to sea level (which has a more pronounced obliquity signal).

Also interesting is the similarity between our conclusions and those of Paillard and Parrenin (2004). These authors developed a conceptual model, which assumes that the glacial reduction in CO_2 depends on storage in the deep ocean driven by stratification in the glacial deep ocean. This stratification is suggested to depend on processes of deep water formation in the Southern Ocean. Therefore these authors developed a threshold parameter with glacial and interglacial states, which determines the efficiency of formation of salty bottom water. The function determining this threshold parameter depends on global ice volume, the extent of the Antarctic ice sheet and Spring insolation at $60°S$. These parameters essentially determine the shelf space available for deep water formation and thereby the switch between relatively light, warm and fresh interglacial deep water formation and cold, salty, dense glacial deep water formation. The switch in state of this parameter occurs only at glacial terminations and inceptions and bears a very close similarity to the deep Pacific temperature time series shown in Fig. 1C.

A more complete analysis of the links with deep Pacific temperature and atmospheric CO_2 concentrations is beyond the remit of this contribution but we hope that our results will inspire modeling efforts linking deep ocean temperature to the carbon cycle. We refer the reader to Hubertus et al., (2010) for a more detailed discussion.

As well as links between deep water formation and GHGs, other mechanisms suggest a link between deep Pacific temperature and atmospheric change. Several authors have noted a cooling in upwelling regions in the south-east of the Atlantic and Pacific basins during the MPT (Marlow et al., 2000; Liu and Herbert, 2004). These authors suggest that the intensification of El Niño/Southern Oscillation (ENSO) may be linked to changes in the meridional transport of heat and water vapor in the atmosphere and might thereby represent an important factor during the glacial cycles of the last 700 kyr. We suggest that the cooling of the eastern Atlantic and Pacific basins is in line with the deep Pacific temperature residuals calculated here because cooler deep Pacific temperatures would affect surface temperatures in the SW Pacific and equatorial upwelling regions. This implies that the non-linear response in deep Pacific temperatures over the glacial cycles may impact ice-sheet formation because of the impact of deep ocean temperature on ENSO variability. Indeed Clark et al. (2007) link the fluctuations in the volume of the Laurentide ice sheet to surface ocean temperature in the equatorial Pacific. Fig. 1D compares sea surface Mg/Ca temperature reconstruction from the south-east Pacific of Wara et al. (2005) with our deep Pacific temperature reconstruction. The change in temperature over the last 2 Ma is both coincident with our deep Pacific reconstruction and of a similar magnitude (2 °C). This agreement also lends support to the argument that changes in the deep Pacific may influence the strength and frequency of the ENSO climate modulation.

4.4. Assumptions

Here we examine the reliability of the assumptions behind the transfer function defined in Section 2.3.

Our method takes data from a small number of MISs (concentrated on the last two glacial cycles). We assume that the transfer function is valid for other periods than the MISs used for the transfer function. To test this assumption we compare our sea-level reconstruction with the independent reconstruction of Siddall et al. (2003) which is based on the deterministic modeling of the relationship between Red Sea oxygen isotopes and sea level and covers the last four glacial cycles (Fig. 1B). Despite differences in age models, the comparison is good, indicating that the transfer function is accurate for at least the last four glacial cycles (i.e. outside of the time window used to constrain the transfer function).

We also assume that the scaling factor used to convert ice-sheet growth/loss into ocean mean enrichment in oxygen isotopes is constant over time. The benthic oxygen isotope values in the deep Pacific follow the global mean change for a given change in ice volume for sea levels below those of MIS 5a (-15.5 ± 1.5 m). This can be seen in Fig. 2 where the benthic oxygen isotope values follow the isotherms. If there were considerable variation in the scaling factor at different stages of ice sheet growth then it would be difficult to explain this result. Although changes in local water mass distributions also affect the benthic oxygen-isotope record, this effect is generally considered to be unimportant in the deep Pacific (Waelbroeck et al., 2002). Furthermore, it is difficult to conceive how the benthic oxygen isotope values would follow the isotherms during the glacial period if hydrographic changes were an important issue.

To further test the assumption that the scaling factor is constant with respect to ice-sheet growth/loss, we compare the residual temperatures from the deep Pacific calculated here with independent temperature estimates. We use temperature measurements from the EPICA Dome C ice core (Jouzel et al., 2007), PMIP 2 (Jansen et al., 2007) and Mg/Ca estimates from the deep Pacific, which allow for uncertainty due to varying deep-sea carbonate-ion concentrations (Lear, 2007) (Fig. 6). Because of the size and relative homogeneity of the modern deep Pacific, temperature changes in the deep Pacific are often considered representative of global temperature change (Lear et al., 2000, 2008) (with the exception of the glacial period, as discussed here). For the purpose of this tentative comparison we adjust the EPICA Dome C temperature estimates assuming an approximate polar amplification factor of two (Hansen et al., 2007). Note that we intend this to be a tentative check of our approach in anticipation of further work in the future and recognize that assuming a constant polar amplification factor may be incorrect (e.g. Masson-Delmotte et al., 2006). Fig. 6 indicates that our assumption of a constant scaling factor with respect to ice-sheet growth/loss is valid to within the uncertainty of the available data. Note that the comparison in Fig. 6 covers data apart from the MISs that were used for the transfer function and therefore also supports this relationship outside of the periods used to generate the transfer function.

5. Conclusions

Our results indicate that driving the MPT deep Pacific temperature and sea level became increasingly decoupled during glacial periods. A notable feature of these results is that we find that the MPT is a continuum to an asymptote of cold, stable deep Pacific temperature during glacial periods. Over subsequent glacial periods the cold, stable deep Pacific temperatures tend to endure longer until there is a transition from predominantly 41-kyr to 100-kyr variability. Both sea level and deep Pacific temperature time series and spectra differ during the last 700 kyr because the deep Pacific temperature reaches a baseline during the glacial periods below which deep Pacific temperature does not fall. This implies that Pacific benthic oxygen isotopes may provide a record of ice-

volume fluctuations during glacial periods. However, during glacial transitions and interglacial periods both temperature and ice volume affect Pacific benthic oxygen-isotope records. Prior to the MPT the benthic isotopes faithfully reflect ice volume and temperature in tandem but afterwards there is a sharp distinction between the patterns of variability.

That the deep Pacific temperature shows such a strikingly non-linear response to orbital forcing suggest it might be a fundamental component behind the 100-kyr variability. In agreement with Shackleton (2000), we suggest that this non-linearity in deep ocean temperature may be linked to GHGs. Our current knowledge of the processes driving glacial to interglacial CO_2 variability rules out firm conclusions in this regard. However, it may be that the 'switch' in deep ocean temperature on 100-kyr time scales influences the timing of glacial to interglacial CO_2 variability. This suggestion bears important similarities with the conceptual model of Paillard and Parrenin (2004). We have also discussed a possible link between deep ocean temperature and meridional heat and moisture transport in the atmosphere linked to the resulting effect on the temperature of upwelled water masses and ENSO. These suggestions point to the potential for the modeling of the ENSO and atmospheric CO_2 response to colder glacial deep Pacific temperatures.

Acknowledgements

References

Adkins, J.F., McIntyre, K., Schrag, D.P., 2002. The salinity, temperature and $\delta^{18}O$ content of the glacial deep ocean. Science 298, 1769–1773.

Adkins, J.F., Schrag, D.P., 2001. Pore fluid constraints on past deep-ocean temperature and salinity. Geophysical Research Letters 28, 771–774.

Antonioli, F., Bard, E., Potter, E.-K., Silenzi, S., Improta, S., 2004. 215-ka History of sea-level oscillations from marine and continental layers in Argenterola Cave speleothems (Italy). Global and Planetary Change 43 (1-2), 57–78.

Antonioli, F., Anzidei, M., Lambeck, K., Auriemma, R., Gaddi, D., Furlani, S., Orrù, P., Solinas, E., Gaspari, A., Karinja, S., Kovačić, V., Surace, L., 2007. Sea level change during Holocene from Sardinia andnortheastern Adriatic (Central Mediterranean sea) from archaeological and geomorphological data. Quaternary Science Reviews 26, 2463–2486.

Bamber, J.L., Ekholm, S., Krabill, W.B., 2001. A new, high-resolution digital elevation model of Greenland fully validated with airborne laser altimeter data. Journal of Geophysical Research 106 (B4), 6733–6745.

Bard, E., Hamelin, B., Fairbanks, R.G., Zindler, A., Arnold, M., Mathieu, G., 1990. U/Th and ^{14}C ages of corals from Barbados and their use for calibrating the ^{14}C time-scale beyond 9000 years BP. Nuclear Instruments and Methods B 52, 461–468.

Bard, E., Antonioli, F., Silenzi, S., 2002. Sea level during the penultimate interglacial period based on a submerged stalagmite from Argenterola Cave, Italy. Earth and Planetary Science Letters 196, 135–146.

Bassett, S.E., Milne, G.A., Mitrovica, J.X., Clark, P.U., 2005. Ice sheet and solid earth influences on far-field sea-level histories. Science 309, 925–928.

Berger, A., Li, X.S., Loutre, M.F., 1999. Modeling northern hemisphere ice volume over the last 3 Ma. Quaternary Science Reviews 18, 1–11.

Bintanja, R., van de Wal, R.S.W., Oerlemans, J., 2005. Modelled atmospheric temperatures and global sea levels over the past million years. Nature 437, 125–128.

Bintanja, R., van de Wal, R.S.W., 2008. North American ice-sheet dynamics and the onset of 100,000-year glacial cycles. Nature 454, 869–872.

Chappell, J., 2002. Sea level changes forced ice breakouts in the Last Glacial Cycle: new results from coral terraces. Quaternary Science Reviews 21 (10), 1229–1240.

Chappell, J., Shackleton, N.J., 1986. Oxygen isotopes and sea-level. Nature 324 (6093), 137–140.

Clark, P.U., Archer, D., Pollard, D., Blum, J.D., Rial, J.A., Brovkin, V., Mix, A.C., Pisias, N.G., Roy, M., 2006. The Middle Pleistocene transition: characteristics, mechanisms, and implications for long-term changes in atmospheric pCO2. Quaternary Science Reviews 25, 3150–3184.

Clark, P.U., Hostetler, S.W., Pisias, N.G., Schmittner, A., Meissner, K.J., 2007. Mechanisms for a ~7-kyr climate and sea-level oscillation during Marine Isotope

Stage 3. In: Schmittner, A., Chiang, J., Hemmings, S. (Eds.), Ocean Circulation: Mechanisms and Impacts. Geophysical Monograph Series, vol. 173. AGU, Washington, D. C, pp. 209–246.

Clark, P.U., Pollard, D., 1998. Origin of the Middle Pleistocene transition by ice sheet erosion of regolith. Paleoceanography 13, 1–9.

Curry, W.B., Oppo, D.W., 2005. Glacial water mass geometry and the distribution of $\delta^{13}C$ of CO_2 in the western Atlantic Ocean. Paleoceanography 20, PA1017. doi:10.1029/2004PA001021.

Cutler, K.B., Edwards, R.L., Taylor, F.W., Cheng, H., Adkins, J., Gallup, C.D., Cutler, P.M., Burr, G.S., Bloom, A.L., 2003. Rapid sea-level fall and deep-ocean temperature change since the last interglacial period. Earth and Planetary Science Letters 206 (3-4), 253–271.

Dansgaard, W., 1964. Stable isotopes in precipitation. Tellus 16 (4), 436–468.

de Garidel-Thoron, T., Rosenthal, Y., Bassinot, F., Beaufort, L., 2005. Stable sea surface temperatures in the western Pacific warm pool over the past 1.75 million years. Nature 433, 294–298.

Duplessy, J.-C., Labeyrie, L., Waelbroeck, C., 2002. Constraints on the ocean oxygen isotopic enrichment between the Last Glacial Maximum and the Holocene: Paleoceanographic implications. Quaternary Science Reviews 21 (1–3), 315–330.

Elderfield, H., Bertram, C.J., Erez, J., 1996. A biomineralization model for the incorporation of trace elements into foraminiferal calcium carbonate. Earth and Planetary Science Letters 142, 409–423.

Emiliani, C., 1955. Pleistocene temperatures. Journal of Geology 63, 585–599.

Fairbanks, R.G., 1989. A 17,000 year glacio-eustatic sea level record: influence of glacial melting rates on the Younger Dryas event and deep ocean circulation. Nature 342, 637–642.

Gallup, C.D., Edwards, R.L., Johnson, R.G., 1994. The timing of high sea levels over the past 200,000 years. Science 263, 796–800.

Hansen, J., Sato, M., Karecha, P., Russel, G., Lea, D.W., Siddall, M., 2007. Climate change and trace gases. Philosophical Transactions of the Royal Society A 365, 1925–1954.

Hubertus, F., Schmitt, J., Lüthi, D., Tschumi, T., Parekh, P., Joos, F., Stocker, T.F., Köhler, P., Völker, C., Gersonde, R., Barbante, C., Le Floch, M., Raynaud, D., Barnola, J.-M., Chappellaz, J., Wolff, E.W., 2010. The role of Southern Ocean processes in orbital and millennial CO_2 variations – a synthesis. Quaternary Science Reviews 29, 193–205.

Huybers, P., 2007. Glacial variability over the last 2 Ma: an extended depth-derived agemodel, continuous obliquity pacing, and the Pleistocene progression. Quaternary Science Reviews 26, 37–55.

Huybers, P., Wunsch, C., 2005. Obliquity pacing of the late Pleistocene glacial terminations. Nature 434, 491–494.

Jansen, E., Overpeck, J., Briffa, K.R., Duplessy, J.-C., Joos, F., Masson-Delmotte, V., Olago, D., Otto-Bliesner, B., Peltier, W.R., Rahmstorf, S., Ramesh, R., Raynaud, D., Rind, D., Solomina, O., Villalba, R., Zhang, D., 2007. Palaeoclimate. In: Solomon, S., Qin, D., Manning, M., Chen, Z., Marquis, M., Averyt, K.B., Tignor, M., Miller, H.L. (Eds.), Climate Change 2007: The Physical Science Basis. Contribution of Working Group I to the Fourth Assessment Report of the Intergovernmental Panel on Climate Change. Cambridge University Press, pp. 433–497.

Jouzel, J., Masson-Delmotte, V., Cattani, O., Dreyfus, G., Falourd, S., Hoffmann, G., Minster, B., Nouet, J., Barnola, J.M., Chappellaz, J., Fischer, H., Gallet, J.C., Johnsen, S., Leuenberger, M., Loulergue, L., Luethi, D., Oerter, H., Parrenin, F., Raisbeck, G., Raynaud, D., Schilt, A., Schwander, J., Selmo, E., Souchez, R., Spahni, R., Stauffer, B., Steffensen, J.P., Stenni, B., Stocker, T.F., Tison, J.L., Werner, M., Wolff, E.W., 2007. Orbital and millennial Antarctic climate variability over the last 800 000 years. Science 317, 793–796. doi:10.1126/science.1141038.

Köhler, P., Bintanja, R., 2008. The carbon cycle during the mid Pleistocene transition: the southern ocean decoupling hypothesis. Climate of the Past 4, 311–332. SRef-ID:1814-9332/cp/2008-4-311.

Labeyrie, L.D., Duplessy, J.C., Blanc, P.L., 1987. Variations in mode of formation and temperature of oceanic deep waters over the past 125,000 years. Nature 327, 477–482.

Lawrence, K.T., Liu, Z., Herbert, T.D., 2006. Evolution of the eastern Tropical Pacific through Plio-Pleistocene glaciation. Science 312, 79–83.

Lear, C.H., 2007. Mg/Ca palaeothermometry: a new window into Cenozoic climate change. In: Haywood, W.M. (Ed.), Perspectives on Climate Change: Marrying the Signal from Computer Models and Biological Proxies. The Micropalaeontological Society, Special Publications, vol. 313–322. The Geological Society, London, p. 2007.

Lear, C.H., Elderfield, H., Wilson, P.A., 2000. Cenozoic deep-sea temperatures and global ice volumes from Mg/Ca in benthic foraminiferal calcite. Science 287, 269–272.

Lear, C.H., Bailey, T.R., Pearson, P.N., Coxall, H.K., Rosenthal, Y., 2008. Cooling and ice growth across the Eocene-Oligocene transition, Geology 36, 251–254.

Lisiecki, L.E., Raymo, M.E., 2005. A Pliocene–Pleistocene stack of 57 globally distributed benthic delta O-18 records. Paleoceanography 20 (1), PA1003.

Lisiecki, L., Raymo, M.E., 2007. Plio-Pleistocene climate evolution: trends in obliquity and precession responses. Quaternary Science Reviews 26, 56–69.

Liu, Z., Herbert, T.D., 2004. High-latitude influence on the eastern equatorial Pacific climate in the early Pleistocene epoch. Nature 427, 720–723.

Lunt, D.J., Foster, G.L., Haywood, A.M., Stone, E.J., 2008. Late Pliocene Greenland glaciation controlled by a decline in atmospheric CO_2 levels. Nature 454, 1102–1105.

Lythe, M.B., Vaughan, D.G., the BEDMAP Consortium, 2001. BEDMAP: a new ice thickness and subglacial topographic model of Antarctica. Journal of Geophysical Research 106 (B6), 11335–11351.

Marlow, J.R., Lange, C.B., Wefer, G., Rosell-Mele, A., 2000. Upwelling intensification as part of the Pliocene–Pleistocene climate transition. Science 290, 2288–2291.

Martin, P.A., Lea, D.W., Rosenthal, Y., Shackleton, N.J., Sarnthein, M., Papenfuss, T., 2002. Quarternary deep sea temperature histories derived from benthic foraminiferal Mg/Ca. Earth and Planetary Science Letters 198 (1–2), 193–209.

Martinson, D.G., Pisias, N.G., Hays, J.D., Imbrie, J., Moore Jr., T.C., Shackleton, N.J., 1987. Age dating and the orbital theory of the ice ages development of a high-resolution 0 to 300 000-year chrostratigraphy. Quaternary Research 27, 1–29.

Masson-Delmotte, et al., 2006. Past and future polar amplification of climate change: climate model intercomparisons and ice-core constraints. Climate Dynamics 26, 513–529.

Meehl, G.A., Stocker, T.F., Collins, W.D., Friedlingstein, P., Gaye, A.T., Gregory, J.M., Kitoh, A., Knutti, R., Murphy, J.M., Noda, A., Raper, S.C.B., Watterson, I.G., Weaver, A.J., Zhao, Z.-C., 2007. Global climate projections. In: Solomon, S., Qin, D., Manning, M., Chen, Z., Marquis, M., Averyt, K.B., Tignor, M., Miller, H.L. (Eds.), Climate Change 2007: The Physical Science Basis. Contribution of Working Group I to the Fourth Assessment Report of the Intergovernmental Panel on Climate Change. Cambridge University Press, Cambridge, United Kingdom and New York, NY, USA.

Miller, K.G., Kominz, M.A., Browning, J.V., Wright, J.D., Mountain, G.S., Katz, M.E., Sugarman, P.J., Cramer, B.S., Christie-Blick, N., Pekar, S.F., 2005. The Phanerozoic record of global sea-level change. Science 312, 1293–1298.

Monnin, E., Indermühle, A., Dällenbach, A., Flückiger, J., Stauffer, B., Stocker, T.F., Raynaud, D., Barnola, J.-M., 2001. Atmospheric CO_2 concentrations over the last glacial termination. Science 291 (5501), 112–114.

Oerlemans, J., Van der Veen, C.J., 1984. Ice Sheets and Climate. Reidel, Dordrecht, 217 pp.

Paillard, D., 1998. The timing of Pleistocene glaciations from a simple multiple-state climate model. Nature 391, 378–381.

Paillard, D., Parrenin, F., 2004. The Antarctic ice sheet and the triggering of deglaciations. Earth and Planetary Science Letters 227 (3–4), 263–271.

Peltier, W.R., Fairbanks, R.G., 2006. Global glacial ice volume and Last Glacial Maximum duration from an extended Barbados sea level record. Quaternary Science Reviews 25, 3322–3337.

Pisias, N.G., Moore Jr., T.C., 1981. The evolution of the Pleistocene climate: a time series approach. Earth and Planetary Science Letters 52, 450–458.

Raymo, M.E., Lisiecki, L., Nisancioglu, K., 2006. Plio-Pleistocene ice volume, Antarctic climate, and the global $\delta^{18}O$ record. Science 313, 492–495. doi:10.1126/science.1123296.

Rial, J.A., 2004. Abrupt climate change: chaos and order at orbital and millennial scales. Global and Planetary Change 41, 95–109.

Rohling, E.J., Grant, K., Hemleben, Ch., Siddall, M., Hoogakker, B.A.A., Bolshaw, M., Kucera, M., 2008. High rates of sea-level rise during the last interglacial period. Nature Geosciences 1, 38–42.

Schellmann, G., Radtke, U., 2004. A revised morpho- and chronostratigraphy of the late and middle Pleistocene coral reef terraces on Southern Barbados (West Indies). Earth-Science Reviews 64, 157–187.

Shackleton, N.J., 1967. Oxygen isotope analyses and Pleistocene temperatures reassessed. Nature 215, 15–17.

Shackleton, N.J., 1974. Attainment of isotopic equilibrium between ocean water and benthic foraminifera genus Uvigerina: isotopic changes in the ocean during the last glacial. Les méthodes quantitatives d' étude des variations du climat au cours du Pleistocne, Gif-sur-Yvette. Colloque international du CNRS 219, 203–210.

Shackleton, N.J., 2000. The 100,000 year ice-age cycle identified and found to lag temperature, carbon dioxide and orbital eccentricity. Science 289, 1897–1902.

Shackleton, N.J., Berger, A., Peltier, W.R., 1990. An alternative astronomical calibration on the Lower Pleistocene time scale based on ODP site 677. Transactions of the Royal Society of Edinburgh, Earth Sciences 81, 2511–3261.

Siddall, M., Rohling, E.J., Almogi-Labin, A., Hemleben, Ch., Meischner, D., Schmelzer, I., Smeed, D.A., 2003. Sea-level fluctuations during the last glacial cycle. Nature 423, 853–858.

Siddall, M., Chappell, J., Potter, E.-K., 2006. Eustatic sea level during past Interglacials. In: Sirocko, F., Litt, T., Claussen, M., Sanchez-Goni, M.-F. (Eds.), The Climate of Past Interglacials. Elsevier, Amsterdam.

Siddall, M., Rohling, E.J., Thompson, W.G., Waelbroeck, C., 2008a. MIS 3 sea-level fluctuations: data synthesis and new outlook. Reviews of Geophysics 46, RG4003. doi:10.1029/2007RG000226.

Siddall, M., Rohling, E.J., Arz, H.W., 2008b. Convincing evidence for rapid ice sheet growth during the last glacial period. PAGES Newsletter 16 (1), 15–16.

Skinner, L.C., Elderfield, H., 2007. Rapid fluctuation in the deep North Atlantic heat budget during the last glaciation. Paleoceanography 22, PA1205. doi:10.1029/2006PA001338.

Skinner, L.C., Shackleton, N.J., 2005. Deconstructing Terminations I and II: revisiting the glacioeustatic paradigm based on deep-water temperature estimates. Quaternary Science Reviews 25 (23–24), 3312–3321.

Stirling, C.H., Esat, T.M., Lambeck, K., McCulloch, M.T., 1998. Timing and duration of the last interglacial: evidence for a restricted interval of widespread coral reef growth. Earth and Planetary Science Letters 160, 745–762.

Thompson, W.G., Goldstein, S.L., 2005. Open-system coral ages reveal persistent suborbital sea-level cycles. Science 308 (5720), 401–404.

Thompson, W.G., Goldstein, S.L., 2006. A radiometric calibration of the SPECMAP timescale. Quaternary Science Reviews 25 (23–24), 3207–3215.

Tziperman, E., Gildor, H., 2003. On the mid-Pleistocene transition to 100-kyr glacial cycles and the asymmetry between glaciation and deglaciation times. Paleoceanography 18.

Waelbroeck, C., Labeyrie, L., Michel, E., Duplessy, J.C., McManus, J.F., Lambeck, K., Balbon, E., Labracherie, M., 2002. Sea-level and deep water temperature changes derived from benthonic foraminifera isotopic records. Quaternary Science Reviews 21, 295–305.

Wara, M.W., Ravelo, A.C., Delaney, M.L., 2005. Permanent El Niño-Like conditions during the Pliocene warm period. Science 309 (5735), 758–761. doi:10.1126/science.1112596.

Wunsch, C., 2003. The spectral description of climate change including the 100 ky energy. Climate Dynamics 20, 353–363. doi:10.1007/s00382-002-0279-z.

Yokoyama, Y., Lambeck, K., De Deckker, P., Johnston, P., Fifield, L.K., 2000. Timing of the Last Glacial Maximum from observed sea-level minima. Nature 406 (6797), 713–716.

Yokoyama, Y., Esat, T.M., Lambeck, K., 2001. Coupled climate and sea-level changes deduced from Huon Peninsula coral terraces of the last ice age. Earth and Planetary Science Letters 193 (3–4), 579–587.

Yu, J., Elderfield, H., 2008. Mg/Ca in the benthic foraminifera Cibicidoides wuellerstorfi and Cibicidoides mundulus: temperature versus carbonate ion saturation. Earth and Planetary Science Letters 276, 129–139.